Al-Azhar University Journal
for Virus Research and Studies

The Possible Protective Effect of Resveratrol Alone or in Combination with Metformin on Diabetic Cardiomyopathy in Adult Male Rats

Azza S. Khalil[1], Samah E. Ibrahim[1*], Rehab A. Hassan[2] and Hanan F. Al-Saeed[1]

[1]Physiology Department, Faculty of Medicine for Girls, Al-Azhar University, Cairo, Egypt.

[2]Histology and Cell Biology Department, Faculty of Medicine for Girls, Al-Azhar University, Cairo, Egypt.

***Email: samah.m.ibrahim24@gmail.com, samahelmetwally.medg@azhar.edu.eg.**

Abstract

Diabetes mellitus (DM) is commonly associated with metabolic alterations and various complications. Resveratrol (RSV) is a natural polyphenolic compound with multiple beneficial activities. The current study investigated the potential cardioprotective role of RSV, administered alone or with a standard anti-diabetic drug, metformin (MET), in type 2 diabetic rat model. Type 2 DM was induced in the current study by administration of a high fat diet (HFD) and a single dose of streptozotocin (STZ). Male rats were classified into 5 groups; normal control, diabetic, MET-treated diabetic, RSV-treated diabetic and MET&RSV-treated diabetic rats. Fasting plasma glucose (FPG), plasma insulin, homeostasis model assessment for insulin resistance (HOMA-IR), cardiac injury markers, oxidative/antioxidative stress markers and apoptotic genes expression were measured. Cardiac histopathological study was also performed. Diabetic rats exhibited significant increase in FPG, insulin, HOMA-IR, troponin I, creatine kinase-MB, malondialdehyde as well as glycogen synthase kinase-3β (GSK-3β) and BAX gene expressions, while a significant reduction in reduced glutathione and Bcl-2 gene expression was observed. These changes were coupled by marked histological alterations of the examined cardiac tissue in comparison to the control group. The altered parameters were improved by treatment with MET, RSV, or both. HFD/STZ resulted in characteristic metabolic features of type 2 DM with elevation of markers of cardiac injury, oxidative stress, and apoptosis. Concomitant treatment with MET and RSV revealed synergistic effect in most of studied parameters, demonstrating that RSV could improve the medicinal efficacy of MET.

Key words: Cardiomyopathy, Diabetes mellitus, Metformin, Resveratrol.

1. Introduction

Diabetes mellitus (DM) is a common metabolic disease, defined as hyperglycaemia associated with dysregulation of carbohydrate, fat, and protein metabolism (Assadi et al., 2021) [1]. Diabetic cardiomyopathy (DCM) is a

diabetic complication, in which the myocardial structure and function are altered in absence of hypertension, valvular or coronary artery diseases (Jia et al., 2018) [2]. The pathophysiology of the diabetes-induced cardiac injury is multifactorial. Oxidative stress is a key contributor for cardiac injury, additionally, inflammation, fibrosis, apoptosis, and autophagy have been linked to its pathogenesis (Othman et al., 2017) [3]. Recent studies have evaluated the relationship between the up-regulation of glycogen synthase kinase-3β (GSK-3β) gene expression and cardiomyocyte apoptosis in DCM, providing a novel management of DCM (Wu et al., 2019) [4]. Metformin (MET) is a potent hypoglycaemic drug. It is known to be the first line of diabetes treatment (Kushwah and Gupta, 2018) [5]. Common adverse effects might develop with MET therapy, but the most serious side effect is lactic acidosis, occurring if MET is prescribed inappropriately (Lipska et al., 2011) [6]. Therefore, new drugs and natural compounds are continually being tested for better prevention and treatment of DM or its complications. Resveratrol (RSV), a natural polyphenolic compound, is present in different plants, like grapes, berries, and peanuts (Chang et al., 2016) [7]. Much attention has been paid to RSV because of its pleiotropic activities. It has antioxidant, anti-inflammatory, anti-aging, anti-cancer, and neuro-protective effects (Qiao et al., 2017) [8]. This work was planned to explore the potential cardioprotective efficacy and possible mechanisms of RSV alone or combined with MET in type 2 diabetic rat model.

2. Materials and Methods

2.1 Drugs

- Streptozotocin and resveratrol (Sigma-Aldrich, St Louis, Missori, USA).
- Metformin, Glucophage, (MINAPHARM for pharmaceutical and chemical industries, 10th of Ramadan, Egypt).

2.2 Experimental animals

Fifty adult male albino rats (120-160 g) were used. Rats were housed in stainless-steel cages, 5 rats/cage (25×15×40 cm). They were kept under prevailing room temperature and humidity with a 12 h light/dark cycle for one week for acclimatization. Rats were provided with standard rat chow and water ad libitum. The animal care and procedures were in accordance with animal ethical guidelines. The study was approved by the research ethics committee of faculty of medicine for girls, Al-Azhar University (FMG-IRB). The experiment was conducted in the research laboratory at Al-Azhar University.

2.2.1 Induction of type 2 diabetes mellitus

Type 2 DM (T2DM) was induced in forty rats by feeding HFD (45% Beef tallow) for four weeks followed by a single intra-peritoneal injection of 30 mg/kg STZ dissolved in sodium citrate buffer, pH 4.5 (Zhang et al., 2018) [9]. After 72 hours fasting blood glucose (FBG) level was measured. Rats with FBG above 7.8 mmol/L were considered diabetics (Zhang and Xu, 2018) [10].

2.3 Experimental design and procedures

Rats were divided into five equal groups (10 rats/ group); group I (normal control), group II (Diabetic), group III (MET-treated): diabetic rats treated with MET (100 mg/kg/d) (Sayed et al., 2017) [11], group IV (RSV-treated): diabetic rats treated with RSV (50 mg/kg/d) (Fang et al., 2018) [12] and group V (MET&RSV-treated): diabetic rats treated with MET and RSV concomitantly as in groups III & IV. Drugs were dissolved in distilled water and each rat received 1 ml of the drug solution, calculated according to the estimated body weight. The drugs were given orally by gastric gavages daily and continued for 8 weeks. At the end of the experimental period, fasting blood samples

were collected from retro-orbital sinuses under pentobarbital sodium anaesthesia, then rats were sacrificed, and hearts were removed. Each heart was divided into two halves; one half was used for cardiac biochemical measurements and the other for histopathological examination.

2.4 Biochemical analysis

The plasma was used for determination of the following parameters according to the manufacturer kits:

- Fasting plasma glucose: using rat glucose assay kit.
- Insulin: using rat insulin ELISA kit.
- Homeostasis model assessment for insulin resistance was calculated from: HOMA-IR equation: glucose (mmol/L) X insulin (μIU/L)/22.5 **(Matthews et al., 1985)**. [13]
- Cardiac troponin I (cTnI): using cTnI ELISA kit.
- Creatine kinase-MB (CK-MB): using CK-MB kit.

2.5 Cardiac tissue sampling

Heart specimens were homogenized according to Yu et al. (2012) [14] for estimation of malondialdehyde (MDA) and reduced glutathione (GSH) by special assay kits (Biodiagnostic, 29 Tahreer St., Dokki, Giza, Egypt).

2.6 Real-time quantitative polymerase chain reaction (qPCR)

The determination method of glycogen synthase kinase-3β (GSK 3B), BAX and Bcl-2 genes expression was according to Sayed et al. (2017). [11]

2.6.1 The primer sequence of the genes

- **GSK 3B:** Forward primer: 5′-TACCCATACGATGTTCCAGAT-3
  Reverse primer: 5′-ACCCTGCCCAGGAGTTGCCAC-3′
- **BAX:** Forward primer: 5′ -CCCTGTGCACTAAAGTGCCCC -3
  Reverse primer: 5′-GTCAGATGGACACATGGTG -3’
- **Bcl-2:** Forward primer: 5′ -CTACGAGTGGGATGCTGGAG
  Reverse primer: 5′-GGTCAGATGGACACATGGTG

2.7 Histopathological Examination

2.7.1 Histological Study

Heart tissue were properly fixed in 10% formaldehyde. All heart specimens were prepared and stained with haematoxylin and eosin (H&E) (Bancroft and Gamble, 2002) [15]. Collagen fibres were stained by Masson's trichrome stain (Al-Rasheed et al., 2017) [16]. Specimens were examined under the light microscope (Primo star, ZEISS, China). Photos were taken by a camera (Axiocam ERc 5s, ZEISS, China), at department of histology and cellular biology, FMG, Al-Azhar University.

2.7.2 Morphometric examination

The following morphometric parameters were measured:

1- Cross sectional area of cardiomyocytes (Liu et al., 2018) [17].

2- Area % of the stained collagen fibres (Hasan et al., 2015) [18].

They were determined by using Image J software (National Institute of Health, Bethesda, Maryland, USA). Photos of a calculated distance in micrometre were prepared for a setting scale. Values were converted from pixels to micrometres (Afsar et al., 2017) [19].

2.8 Statistical analysis

Data were statistically analysed using Statistical Package for Social Science software version 25. Comparison of data was done by one-way analysis of variance (ANOVA), followed by post-hoc Tukey test to determine the significant difference between groups. Values were presented as mean and standard deviation (SD). Values

were considered statistically significant when $P \leq 0.05$.

3 .Results

3.1 Biochemical results

Changes in the studied biochemical parameters in different experimental rat groups are demonstrated in Table, 1.

3.1.1 Fasting plasma glucose (FPG), insulin and HOMA-IR

Diabetic rats exhibited a significant increase in FPG, insulin and HOMA-IR, compared to the normal control. Administration of MET or RSV significantly decreased these parameters, compared to the diabetic group. Co-administration of MET and RSV resulted in significant decrease in FPG, plasma insulin and HOMA-IR, compared to diabetic, MET-treated, or RSV-treated groups.

3.1.2 Plasma cardiac troponin I (cTnI) and creatine kinase-MB (CK-MB):

Diabetes induced significant increase in cTnI and CK-MB levels, compared to the control. MET or RSV-treated groups showed significant reduction in cTnI and CK-MB levels, compared to the diabetic group. Co-administration of MET and RSV resulted in significant reduction in cTnI and CK-MB levels, compared to diabetic group. In comparison to either MET or RSV-treated groups, CK-MB in the combined group significantly decreased, while cTnI insignificantly changed. In comparison to the normal control group, CK-MB level in the combined group significantly increased, while cTnI insignificantly changed.

3.1.3 Cardiac malondialdehyde (MDA) and reduce glutathione (GSH):

The diabetic group showed significant increase in of MDA and significant decrease in GSH levels as compared to the control. Administration of MET or RSV resulted in significant decrease of MDA and increase of GSH levels, compared to the diabetic group. Combined administration of MET and RSV resulted in significant decrease in MDA and increase in GSH levels, compared to diabetic, MET-treated, or RSV-treated groups. MDA in the combined group insignificantly changed, while GSH significantly decreased, compared to the normal control group.

3.1.4 Cardiac glycogen synthase kinase-3β (GSK-3β), BAX and BcL-2 gene expressions

The diabetic rats showed significant increase in GSK-3β and BAX gene expressions and significant decrease in Bcl-2 gene expression, compared to the normal control. Administration of MET or RSV significantly decreased GSK-3β and BAX expression and significantly increased Bcl-2 expression, compared to diabetic group. Co-administration of MET and RSV significantly decreased GSK-3β & BAX expression and significantly increased Bcl-2 expression, compared to diabetic, MET-treated, or RSV-treated groups. GSK-3β and BAX genes in the combined group insignificantly changed, while BcL-2 expression significantly decreased, compared to the normal control group.

3.2 Histopathological results

3.2.1 Hematoxylin & Eosin (H&E) stain

The control group showed a typical normal histological structure of the myocardium (Fig. 1, A- B). In longitudinal sections, muscle fibres appeared longitudinally striated, branched, and anastomosed, with acidophilic sarcoplasm and central oval vesicular nuclei. In transverse sections, fibres showed polygonal and polyhedral appearance. The nuclei were central and round.

.

Table (1): Changes in levels of FPG, insulin, HOMA-IR, troponin I, CK-MB, MDA, GSH, BAX gene and Bcl2 gene in experimental groups.

Groups / Parameters	Group I (Normal control)	Group II (Diabetic)	Group III (MET-treated diabetic)	Group IV (RSV-treated diabetic)	Group V (MET&RSV-treated diabetic)
	Mean ± S.D.				
FPG (mmol/l)	3.90± 0.59	17.12±1.88 [a]	9.45 ±1.12[a, b]	8.06 ±0.83[a, b]	5.21 ±1.02[b, c, d]
Insulin (µ IU/l)	6.73±0.45	20.75± 1.71[a]	11.78 ± 1.28[a, b]	11.36± 1.48[a, b]	8.58± 1.28[b, c, d]
HOMA-IR	1.23±0.25	15.68±2.38[a]	4.95±0.77[a, b]	4.27±0.92[a, b]	1.99±0.37[b, c, d]
Troponin I (ng/ml)	0.42±0.10	2.33±0.30[a]	0.90± 0.07[a, b]	0.89± 0.22[a, b]	0.63± 0.14[b]
CK-MB (U/l)	116.23±5.07	284.71±20.58[a]	182.30±19.91[a, b]	183.35±12.19[a, b]	155.38±10.74[a, b, c, d]
MDA (nmol/mg)	38.68±11.37	134.31±12.22[a]	87.48±11.78[a, b]	86.13±9.29[a, b]	59.33±20.08[b, c, d]
GSH (mmol/mg)	83.45±5.37	25.96±4.07 [a]	51.18± 5.79[a, b]	48.00± 6.69[a, b]	68.33±3.46[a, b, c, d]
GSK-3β gene	1.01±0.02	6.38±1.42[a]	3.09±0.31[a, b]	3.17± 0.74[a, b]	1.83±0.21[b, c, d]
BAX gene	1.01±0.01	6.41±1.22[a]	2.80± 0.23[a, b]	2.73± 0.40[a, b]	1.66±0.34[b, c, d]
Bcl-2 gene	1.01±0.01	0.14±0.02[a]	0.61± 0.10[a, b]	0.59± 0.11[a, b]	0.81±0.08[a, b, c, d]

MET-treated= Metformin-treated group, RSV-treated= Resveratrol-treated group, MET&RSV-treated= Metformin & Resveratrol-treated group. The differences between groups were considered statistically significant when P≤0.05. a = significant values versus group I, b= significant values versus group II, c= significant values versus group III, d= significant values versus group IV.

The diabetic group demonstrated marked alteration of cardiac histological structure (Fig. 2, A- B- C). In cut sections, there were cardiomyocyte degeneration, hypertrophy, separated by wide intercellular spaces, dark-stained nuclei. Areas of haemorrhage and mononuclear cell infiltration were observed. Administration of MET (Fig. 3, A- B) or RSV (Fig. 4, A- B) showed improvement in the diabetes-induced cardiomyocyte hypertrophy and significant decrease in the cross-sectional area of cardiomyocytes, Co-administration of MET and RSV (Fig. 5, A-B) showed that the myocardial histological architecture was closely like that of the normal control group, with improvement of the cardiomyocytes hypertrophy and inflammation.

Table (3): Correlation between age and psychological distress, depression, anxiety experienced by study population.

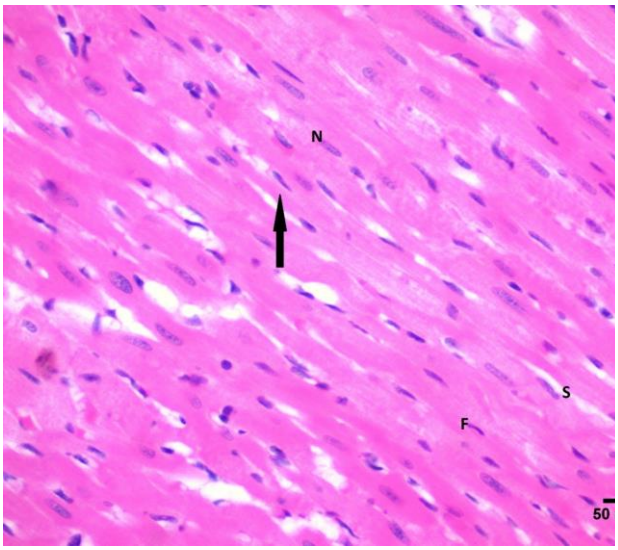

Figure (1 A): A longitudinal section (LS) in fibers of the cardiac muscle of the control rats, demonstrating a normal anastomosing and branching appearance of the fibers (black arrow), acidophilic sarcoplasm and a central oval nucleus (N). Narrow intercellular spaces separate the cardiac muscle fibers(S). The fibroblasts (F) can be seen in the interstitium of the myocytes **(H&E X 400)**.

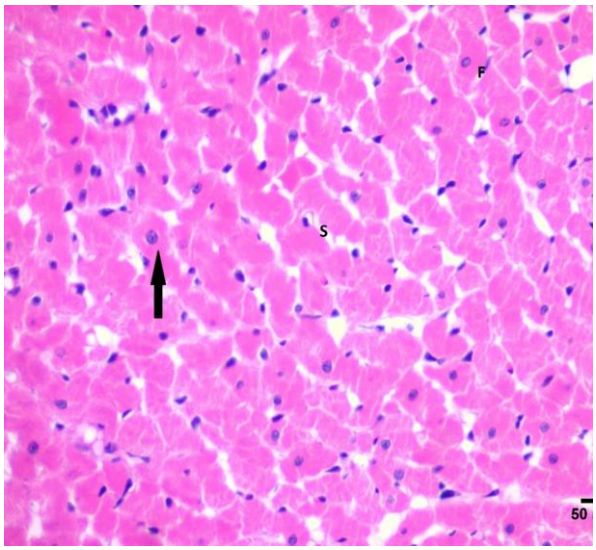

Figure (1 B): A transverse section (TS) in the tissue of the cardiac muscle fiber of the control rats, demonstrating normal shape (polyhedral and polygonal) of the muscle fibers (black arrow) with a central round nucleus. S: Narrow intercellular spaces. F: fibroblasts' nuclei, seen in myocytes' interstitial spaces (H&E X 400).

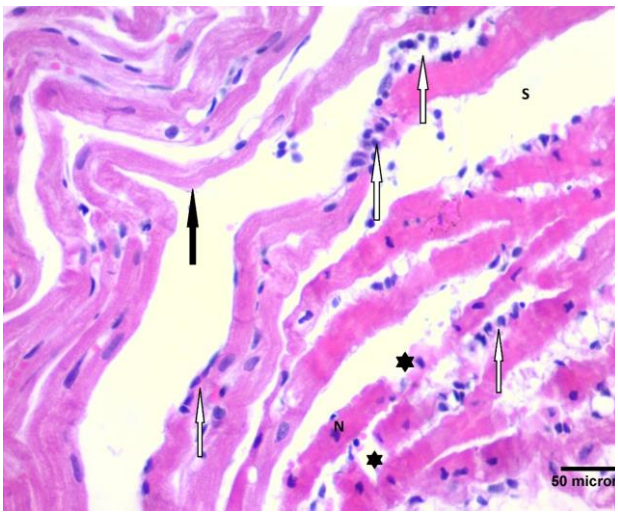

Figure (2 A): A longitudinal section (LS) in fibers of cardiac muscle of the untreated-diabetic rats. The cardiomyocytes appear separated by wide spaces (S). Some cardiomyocytes are irregular and wavy (black arrow) and others appear discontinuous and interrupted (*). Some myocytes nuclei (N) appear darkly stained. Mononuclear cellular infiltration (white arrows) can be seen scattered in multiple areas of the section **(H&E X 400)**.

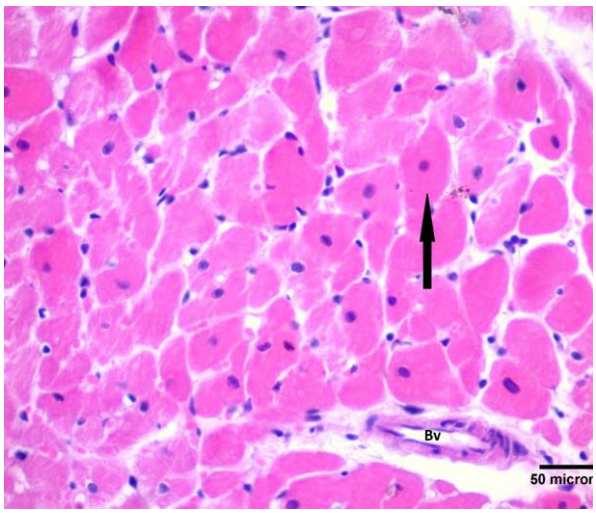

Figure (2 B): A transverse section (TS) in the cardiac muscle fibers of the untreated-diabetic rat group, demonstrating hypertrophied appearance of the cardiomyocytes (black arrow). Dilated blood vessels with thick wall (Bv) can be seen **(H&E X 400)**.

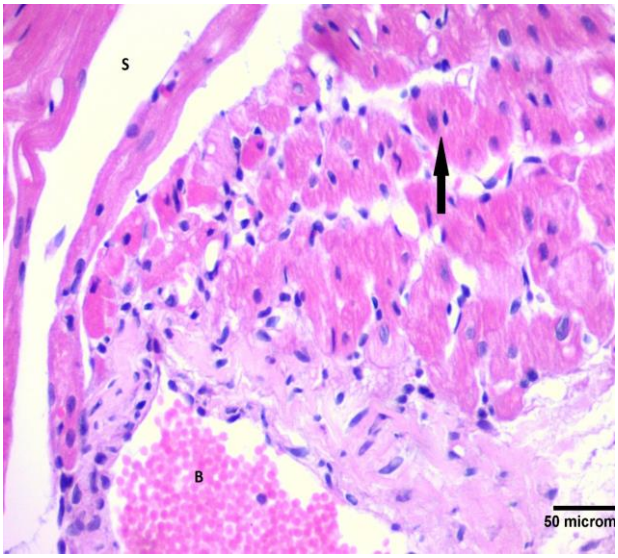

Figure (2 C): A combined longitudinal and transverse section in the cardiac muscle fibers of the untreated-diabetic rat group, demonstrating widely separated cardiomyocytes (S). Many cardiomyocytes appear hypertrophied (black arrow). Extravasated blood (B) can be seen within the section **(H&E X 400)**.

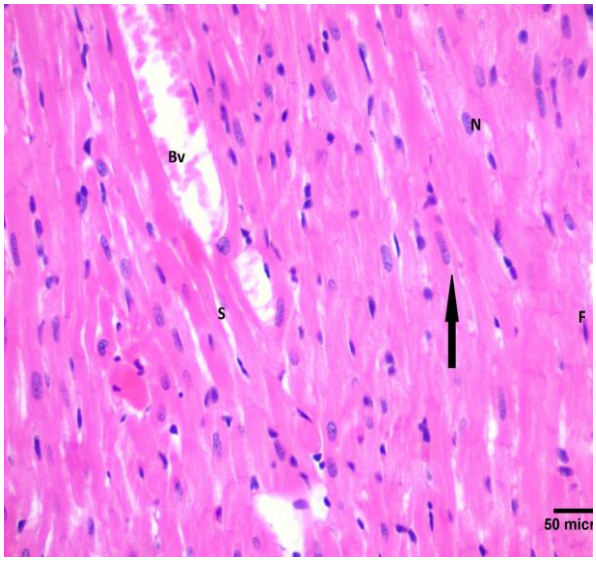

Figure (3 A): A longitudinal section (LS) in tissue of the cardiac muscle fibers of MET-treated rats, demonstrating that the structure of muscle fibers (black arrow) is nearly the same as that in the control group. Some congested and dilated blood vessels (Bv) are found in the section. N: nucleus of a cardiac muscle fiber, S: spaces separate the myocytes, F: nucleus of a fibroblast. **(H&E X 400)**.

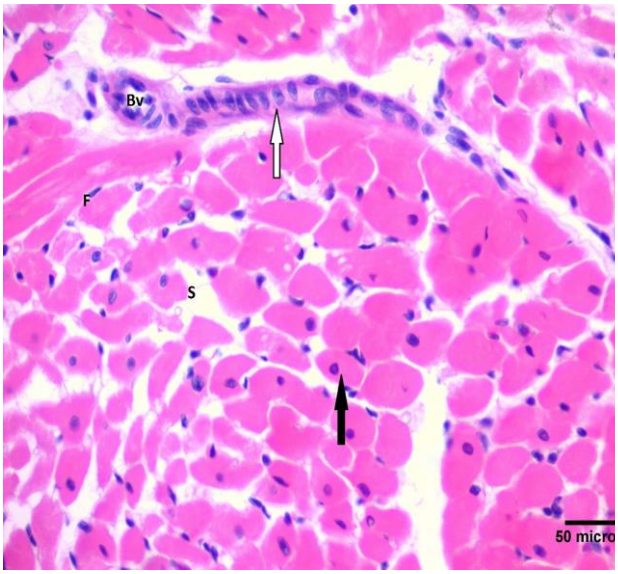

Figure (3 B): A transverse section (TS) in fibers of the cardiac muscle of MET-treated rat group, demonstrating that the tissue structure is nearly the same as the control group. Slightly wide intercellular spaces (S) appear separating the cardiac muscle fibers. The fibroblasts' nuclei (F) were present. Dilated blood vessels (Bv) with thick wall and some mononuclear cell infiltration (white arrow) can be observed **(H&E X 400)**.

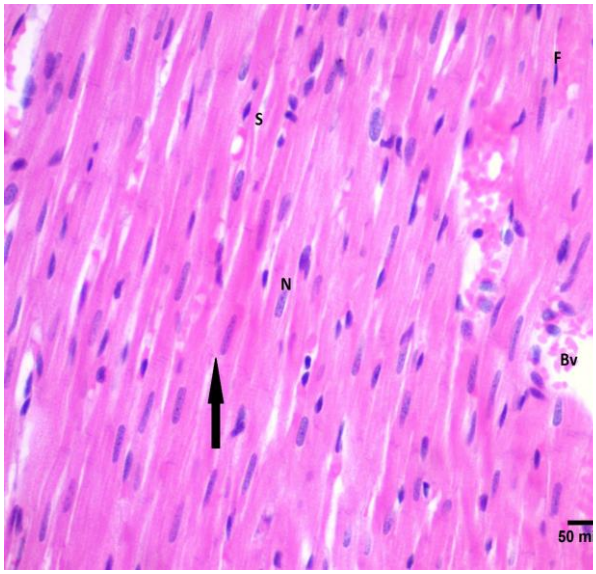

Figure (4 A): A longitudinal section (LS) in fibers of the cardiac muscle of RSV-treated rat group, demonstrating that the tissue structure (black arrow) is nearly the same as that of the control rats. Some dilated and congested blood vessels (Bv) can be noticed. N: nucleus of a cardiac muscle fiber, S: spaces separate the myocytes, F: nucleus of a fibroblast. **(H&E X 400).**

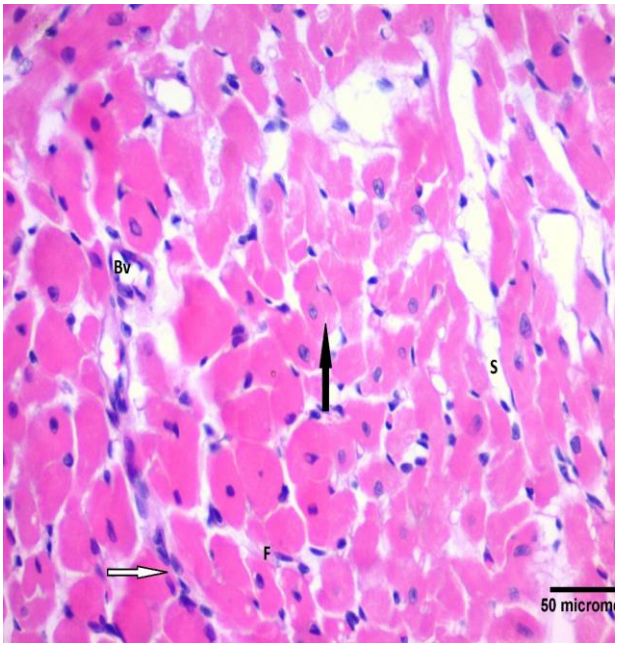

Figure (4 B): A transverse section (TS) in the fibers of the cardiac muscle of RSV-treated rats, demonstrating that muscle structure (black arrow) is nearly the same as that of the control group. Slightly wide intercellular spaces (S) appear separating the cardiac muscle fibers. There are nuclei of fibroblasts (F) seen between the cardiomyocytes. Dilated blood vessels (Bv) with thick wall and some mononuclear cell infiltration (white arrow) still be found **(H&E X 400)**.

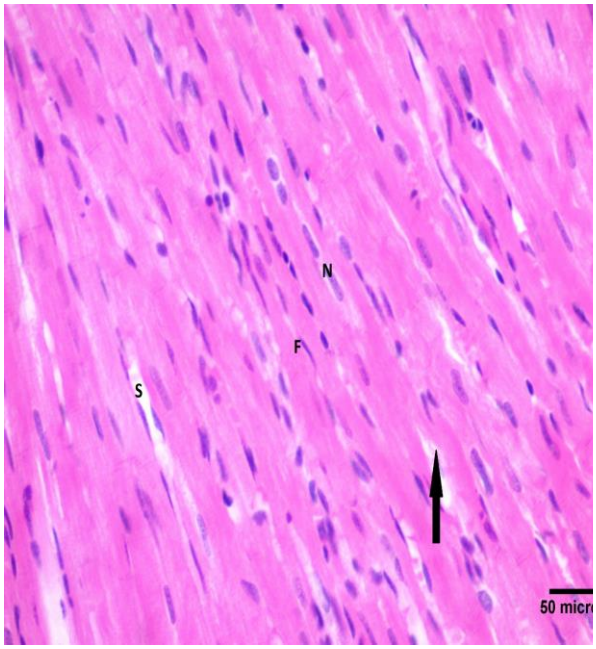

Figure (5 A): A longitudinal section (LS) in fibers of the cardiac muscle of MET&RSV-treated rat group. The tissue structure (arrow) is nearly the same as that of the control rat group. N: nucleus of a cardiac muscle fiber, S: spaces separate the myocytes, F: nucleus of a fibroblast. **(H&E X 400)**.

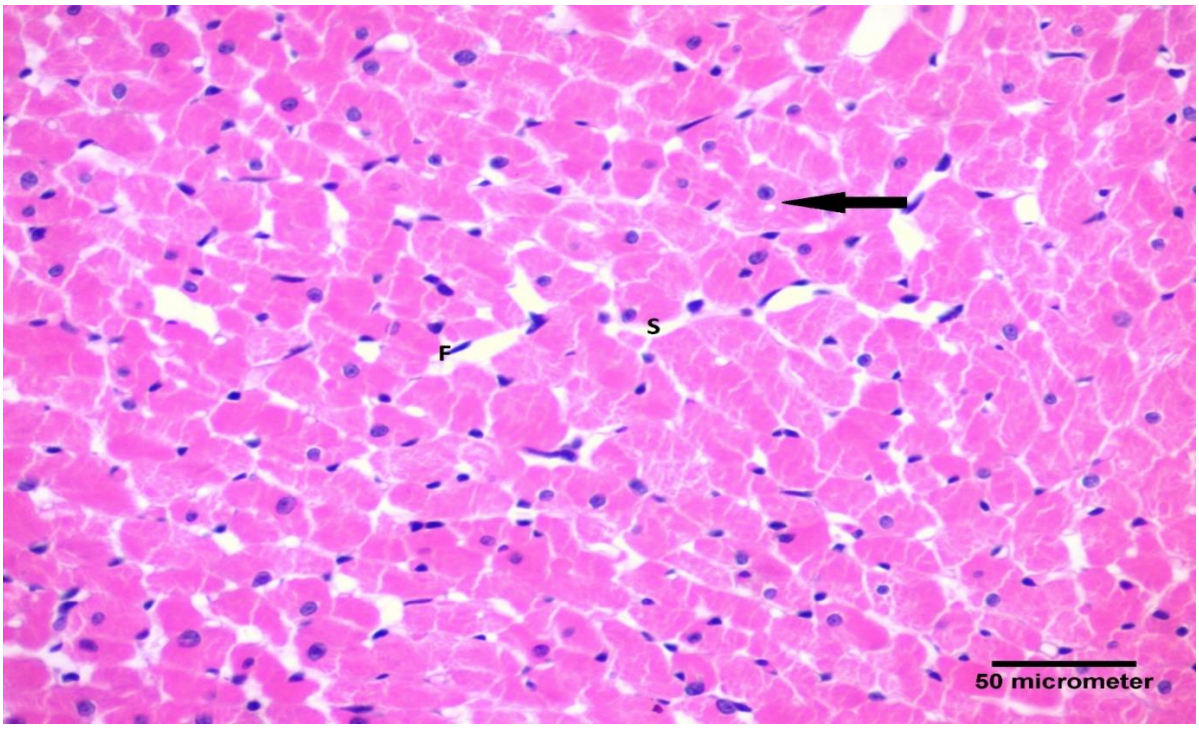

Figure (5 B): A transverse section (TS) in fibers of the cardiac muscle of MET&RSV-treated rat group, demonstrating that the tissue structure (black arrow) is nearly the same as the control rat group. N: nucleus of a cardiac muscle fiber, S: spaces separate the myocytes, F: nucleus of a fibroblast. **(H&E X 400).**

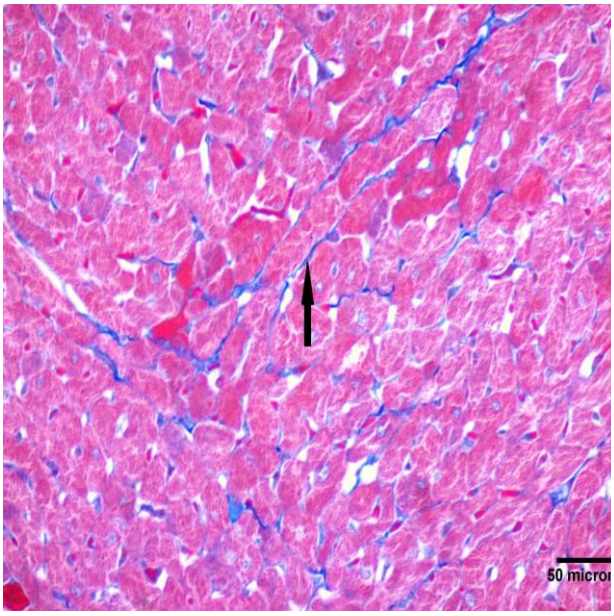

Figure (6): A transverse section (TS) in the fibers of cardiac tissue of the control rat group, demonstrating deposition of few collagen fibers (black arrow) **(Masson's trichrome-stain X 400)**.

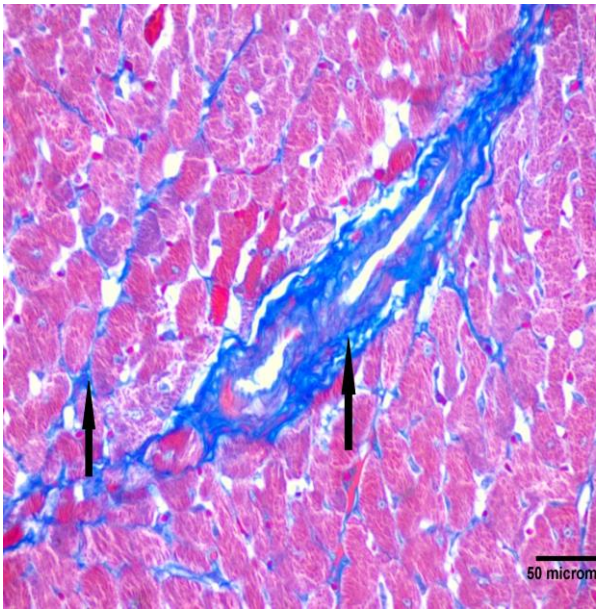

Figure (7): A transverse section (TS) in muscles of cardiac tissue of the untreated-diabetic rat group. Deposition of excessive collagen fibers (black arrows) are seen between the myocytes **(Masson's trichrome- stain X 400)**.

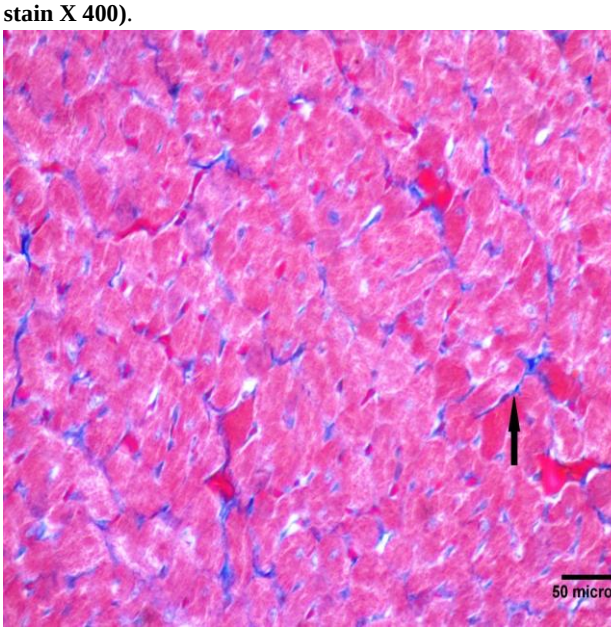

Figure (8): A transverse section (TS) in muscle of cardiac tissue of MET-treated rat group. Deposition of few collagen fibers (black arrow) are seen between the myocytes **(Masson's trichrome- stain X 400)**.

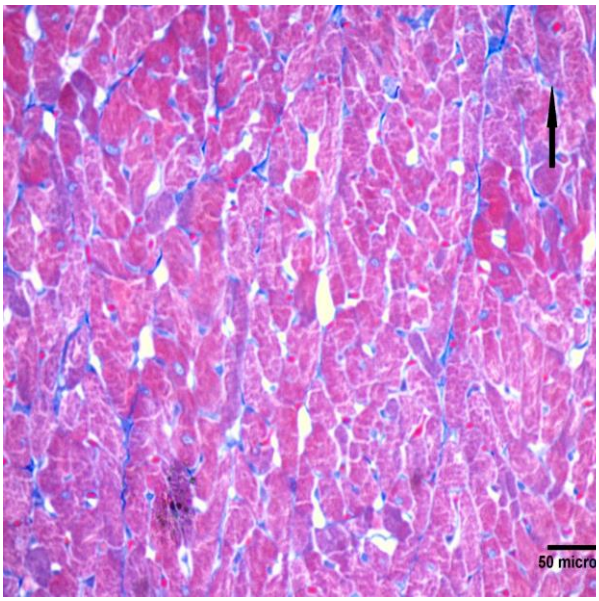

Figure (9): A transverse section (TS) in muscle of cardiac tissue of RSV-treated rat group, illustrating deposition of little collagen fibers (black arrow) seen between the myocytes **(Masson's trichrome - stain X 400)**.

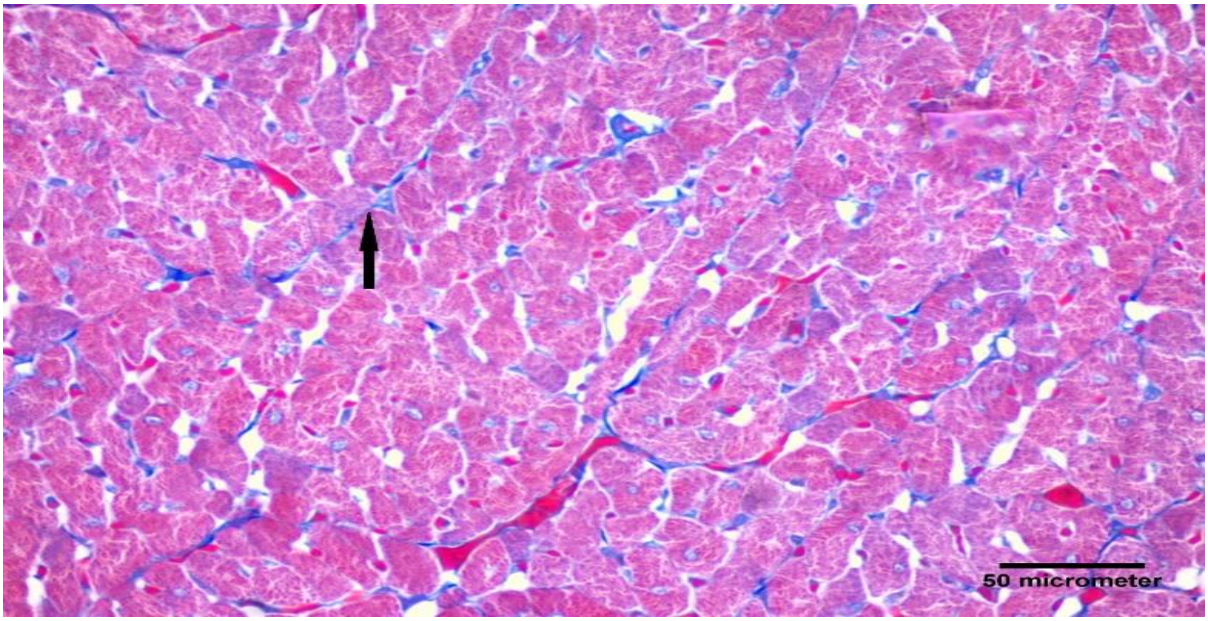

Figure (10): A transverse section (TS) in muscle of cardiac tissue of MET&RSV-treated rat group. Deposition of few collagen fibers (black arrow) are seen (Masson's trichrome- stain X 400).

3.2.2 Masson's trichrome stain

There were few numbers of collagen fibers seen between the cardiomyocytes in the control group (Fig. 6). While sections in the untreated-diabetic group (Fig. 7) showed apparent fibrosis in the interstitial tissue between the cardiomyocytes as well as in perivascular areas. However, following treatment with MET (Fig. 8), RSV (Fig. 9) or both (Fig. 10) there was a marked alleviation of the fibrotic changes in the heart.

3.3 Morphometric measurements

Changes in the cross-sectional area of cardiomyocytes and collagen fibers (%) in different experimental rat groups are demonstrated in Table, 2.

3.3.1 Cross-sectional area of cardiomyocytes (μm^2)

The untreated-diabetic group showed a significant increase in the cross-sectional area of cardiomyocytes, compared to the control group. Administration of MET or RSV showed a significant decrease in the cross-sectional area of cardiomyocytes, compared to the untreated-diabetic group. On the other hand, there was insignificant difference between both treated groups. Co-administration of MET and RSV showed a significant decrease in the cross-sectional area of cardiomyocytes as compared to the untreated-diabetic group. However, it decreased insignificantly as compared to either MET or RSV-treated groups.

3.3.2 Stained collagen fibers(%)

The untreated-diabetic group showed a significant increase in the area % of collagen fibers, compared to the control group. Administration of MET or RSV showed a significant decrease in the area % of collagen fibers, compared to the untreated-diabetic group. On the other hand, there was insignificant difference between both treated groups. Co-administration of MET and RSV showed a significant decrease in the area % of collagen fibers, compared to the untreated-diabetic group. However, it decreased insignificantly, compared to either MET or RSV-treated group.

Table (2): Changes in cross sectional area of cardiomyocytes and area % of collagen in different experimental groups

Groups / Paramete	Group I (Normal control)	Group II (Diabetic)	Group III (MET-treated diabetic)	Group IV (RSV-treated diabetic)	Group V (MET&RSV-treated diabetic)
	Mean ± S.D.				
Cross sectional area of cardiomyocytes (μm^2)	237.41 ±26.85	611.59 ±106.96[a]	303.73 ±55.77[b]	308.16 ±59.54[b]	255.39 ±52.76[b]
Area % of collagen/μm^2	7.34±0.67	25.01± 0.90[a]	7.66 ± 0.57[b]	7.87± 1.09[b]	7.42± 0.64[b]

MET&RSV-treated= Metformin & Resveratrol-treated group. The difference between groups was considered statistically significant when P≤0.05. a= significant values versus group I, b= significant values versus group II.

4. Discussion

In the present study, the untreated-diabetic rats exhibited significant increase in FPG, insulin and HOMA-IR levels. These are in consistency with **Saad et al. (2014) [20]**. Hyperglycemia could be due to the activation of glucose-6-phosphatase and fructose-1,6-bisphosphatase in response to insulin resistance. Insulin is an inhibitor for these enzymes under normal conditions **(Subhasree et al., 2015) [21]**. Treatment with MET significantly decreased these parameters, which is in consistency with **Abdulmalek and Balbaa (2019) [22]**. The effect of MET might be due to inhibition of hepatic glucose production either through impairment of lactate availability as a substrate for gluconeogenesis via inhibiting the mitochondrial glyceraldhyde-3-phosphate dehydrogenase **(Madiraju et al., 2014) [23]** or down-regulating the genes of key enzymes of gluconeogenesis **(Im et al., 2015) [24]**. Additionally, RSV significantly decreased FPG, insulin and HOMA-IR, which agrees with **Diao et al. (2019) [25]**. This was explained by **Wu et al. (2017) [26]** who stated that RSV increases the glucose uptake and subsequent utilization in skeletal muscle cells by enhancing the expression and endogenous trans-location of glucose transporter-4 on the membranes of skeletal muscles. Co-administration of MET and RSV significantly decreased FPG, insulin and HOMA-IR of the diabetic rats. Moreover, these results are significantly lower, in comparison to either MET or RSV-treated groups. This suggests a synergistic effect of both drugs in improvement of glucose metabolism, and this might be due to different mechanisms of drug action. In the present study, plasma cTnI and CK-MB levels significantly increased in diabetic rats. **Bhattacharjee et al. (2016) [27]** proposed that persistent hyperglycaemia provokes excessive formation of reactive oxygen species (ROS), that activates protein kinase C and nuclear factor-κB. The latter induces myocardial injury through release of local inflammatory cytokines. MET and/or RSV decreased cTnI and CK-MB levels significantly. The cardioprotective effect of MET agrees with **Al-Damry et al. (2018) [28]**. **Kobashigawa et al. (2014) [29]** demonstrated such effect and stated that MET can block the mitochondrial permeability transition pores and cytochrome-c release. Additionally, MET induces the cardiac autophagy process and improves cardiac functions.

The exact mechanism of cardioprotective effect of RSV is not clearly known.

Manjunatha et al. (2020) [30] supposed that RSV can conserve the integrity and permeability of myocardial membranes through decreasing lipid peroxidation and via its antioxidant effect. Combined therapy of MET and RSV showed synergistic effect in decreasing CK-MB level, which indicates their positive effect in preserving the cardiac membrane integrity and restricting the leakage of the cardiac enzymes.

Oxidative stress is evidenced in the untreated-diabetic rats of the present study, which is in consistency with **Abdulmalek and Balbaa (2019) [22]**. **Maritim et al. (2003) [31]** proposed that hyperglycaemia leads to free radical production through glucose auto-oxidation, non-enzymatic glycation of proteins and enhancement of lipid peroxidation. MET, RSV or both significantly ameliorated the oxidative stress. MET effects are consistent with **Assadi et al. (2021) [1]**. MET could reduce oxidative stress by inhibiting the production of NADPH oxidase and via increasing the production and activity of antioxidants **(Xu et al., 2020) [32]**.

The antioxidant effect of RSV is in consistency with **Fang et al. (2018) [12]**. It was reported by **Gong et al. (2020) [33]** that RSV serves as a free radical scavenger depending on hydroxyl groups of phenols in its structure. Fortunately, there was a profound synergistic effect of MET and RSV in lowering MDA and elevating GSH levels, which indicates their ability in counteracting the diabetes-associated oxidative stress in cardiac tissue. This may also be owing to their hypoglycemic and potent anti-inflammatory properties.

The present study demonstrated that diabetic rats exhibited significant increase in GSK-3β and BAX expression with significant decrease in Bcl-2 expression. These are in consistency with **Al-Damry et al. (2018) [28]**. The hyperglycaemia-derived ROS plays a crucial role in diabetic cardiac apoptosis as oxidative stress activates various pathways located downstream of the apoptotic signaling pathways in myocardium, including the caspase-3 activation pathway **(El-Missiry et al., 2015) [34]**. While **Wu et al. (2019) [4]** stated that high glucose concentrations inhibit the activation of PI3K/Akt signal transduction pathway in cardiomyocyte, which result in reduced phosphorylation and subsequent up-regulation of GSK-3β gene expression. Treatment with MET and/or RSV significantly improved the apoptotic markers. The anti-apoptotic effect of MET agrees with **Al-Damry et al. (2018) [28]** who referred such effect to the ability of MET in suppressing the lipotoxicity-provoked myocardial apoptosis by its hypolipidemic effect or via elevating the circulating levels of glucagon like peptide-1, which has been known to inhibit cardiac apoptosis.

The antiapoptotic effect of RSV is in consistency with **Diao et al. (2019) [25]**. It was explained by **Hsu et al. (2010) [35]** that RSV can prevent apoptosis via activation of silent information regulator 1 (SIRT1). Increased expression of SIRT1, up-regulates the Bcl-2 expression in myocardial tissue and down-regulates the pro-apoptotic proteins expression, BAX, and cleaved caspase-3, thereby inhibiting cardiomyocyte apoptosis. Co-administration of MET and RSV showed significant effects in decreasing BAX and in increasing Bcl-2 gene expression. We could refer to the resultant effect to their antioxidant and hypoglycaemic effects.

The histological findings in diabetic rats are in consistency with **Othman et al. (2017) [3]** and **Zheng et al. (2019) [36]. Pappachan et al. (2013) [37]** hypothesized that "hyperglycaemia increases the free fatty acids (FFA), especially the saturated FA, palmitate, which causes accumulation of a toxic intermediate, ceramide. Accumulation of palmitate, ceramide and triglycerides in the cardiomyocytes induces oxidative

stress, apoptosis, cardiomyocytes hypertrophy as well as cardiac dysfunction". While **Huynh et al. (2014) [38]** reported that myocardial glucotoxicity, lipotoxicity and over production of reactive oxygen as well as nitrogen species in DM, are the main causes of disruption of cardiac histological structure and functions.

The improvement of deteriorated cardiac histology by MET therapy was also reported by **Abdel-Hamid and Firgany (2018) [39].** The cardioprotective outcome of MET was described by **Asensio-López et al. (2011) [40]** who reported that MET increases the circulating levels of adiponectin and up-regulates its receptors. So, the vasodilator, anti-apoptotic, anti-oxidative and anti-inflammatory effects of adiponectin protect both cardiomyocytes and vascular endothelial cells **(Li et al., 2010) [41].** Additionally, **Yang et al. (2019) [42]** reported that MET improved cardiomyocytes hypertrophy and collagen deposition in the diabetic group. They returned the cardioprotective effect of MET to its ability in activating AMPK/autophagy pathway. Such a pathway promotes the turnover and removal of damaged organelles and protein aggregates.

The protective effect of RSV on cardiac tissue was also reported by **Duarte-Vázquez et al. (2018) [43] and Diao et al. (2019) [25]. Arafa et al. (2014) [44]** stated that RSV confers a cardioprotective effect due to its anti-apoptotic and anti-inflammatory effects that may be partly mediated by down-regulation of toll-like receptor-4/NF-κB signalling pathway for inflammation. **Vasamsetti et al. (2016) [45]** further revealed that the cardiovascular protective effects of RSV might be through its ability in inhibiting the proliferation of smooth muscle cells, oxidation of LDL-C and synthesis of lipids and eicosanoids that promote inflammation and atherosclerosis.

6. Conclusion

Administration of HFD and single low dose of STZ produced hyperglycaemia, hyperinsulinemia, and insulin resistance in adult male rats, which are characteristic features of T2DM. These are accompanied by elevation of markers of cardiac injury, oxidative stress, and apoptotic genes, as well as cardiac alteration and cardiomyocytes degeneration with extensive fibrosis. The present work clearly demonstrated the potentials of RSV on alleviating diabetic cardiomyopathy (DCM). Combination of both MET and RSV revealed synergistic effects in most of the studied parameters, which reveals that addition of RSV could improve the efficacy of MET in T2DM. Further research are needed to reveal other encountered molecular mechanisms of RSV.

Conflict of interest

The authors declare that there are no conflicts of interest.

References

1. Assadi S, Shafiee SM, Erfani M and Akmali M. Antioxidative and antidiabetic effects of Capparis spinosa fruit extract on high-fat diet and low-dose streptozotocin-induced type 2 diabetic rats. Biomedicine & Pharmacotherapy 2021; 138: 111391-111400.
2. Jia G, Hill MA and Sowers JR. Diabetic cardiomyopathy: an up-date of mechanisms contributing to this clinical entity. Circ Res. 2018; 122 (4): 624-638.
3. Othman AI, El-Sawi MR, El-Missiry MA and Abukhalil MH. Epigallocatechin-3- gallate protects against diabetic cardiomyopathy through modulating the cardiometabolic risk factors, oxidative stress, inflammation, cell death and fibrosis in streptozotocin-nicotinamide-

induced diabetic rats: Biomedicine and Pharmacotherapy 2017; 94: 362–373.

4. Wu W, Liu X and Han L. Apoptosis of cardiomyocytes in diabetic cardiomyopathy involves overexpression of glycogen synthase kinase-3β. Bioscience reports 2019; 39(1): 20171307–20171315.
5. Kushwah AS and Gupta GD. Concomitant use of Quercetin and Metformin improve cardiac function and baroreflex sensitivity in Streptozotocin-induced diabetic rats. Asian Journal of Pharmacy and Pharmacology 2018; 4(3): 343-352.
6. Lipska KJ, Bailey CJ and Inzucchi SE. "Use of metformin in the setting of mild-to-moderate renal insufficiency". Diabetes Care 2011; 34(6): 1431-1437.
7. Chang CC, Lin KY, Peng KY, Day YJ and Hung LM. Resveratrol exerts anti-obesity effects in high-fat diet obese mice and displays differential dosage effects on cytotoxicity, differentiation, and lipolysis in 3T3-L1 cells. Endocr J. 2016; 63(2): 169-178.
8. Qiao Y, Gao K, Wang Y, Wang X and Cui B. Resveratrol ameliorates diabetic nephropathy in rats through negative regulation of the p38 MAPK/TGF-β1 pathway. Exp Ther Med. 2017; 13(6): 3223-3230.
9. Zhang Q, Xiao X, Zheng J, Li M, Yu M, Ping F, Wang T and Wang X. Liraglutide protects cardiac functions in diabetic rats through the PPARalpha pathway. Bioscience Reports 2018; 38(2): BSR20180059-20180071.
10. Zhang B and Xu D. Protective effects of astaxanthin on diabetic cardiomyopathy in rats. CyTA - Journal of Food 2018; 16(1): 909-915.
11. Sayed DM, Amin SN, Yassa HD, Rasheed LA, El Tablawy N and Elattar S. Effects of vitamin D and metformin on diabetic cardiomyopathy in rats with type 2 Diabetes Mellitus. International Journal of Anatomy Physiology and Biochemistry 2017; 4(4): 1-13.
12. Fang W, Wang C, He Y, Zhou YL, Peng XD and Liu SK. Resveratrol alleviates diabetic cardiomyopathy in rats by improving mitochondrial function through PGC-1α deacetylation. Acta Pharmacol Sin. 2018; 39(1): 59-73.
13. Matthews D, Hosker J and Rudenski A. Homeostasis model assessment: insulin resistance and beta-cell function from fasting plasma glucose and insulin concentrations. Diabetol. 1985; 28 (7): 412-419.
14. Yu W, Wu J, Cai F, Xiang J and Zha W. Curcumin Alleviates Diabetic Cardiomyopathy in Experimental Diabetic Rats. PLOS ONE 2012; 7(12): e52013-e52023.
15. Bancroft J and Gamble M. Theory and practice of histological techniques. 5th ed. Philadelphia: Churchill Livingstone 2002.
16. Al-Rasheed N, Al-Rasheed N, Hasan I, Al-Amin MA, Al-Ajmi HN, Mohamad RA and Mahmoud AM. Simvastatin ameliorates diabetic cardiomyopathy by attenuating oxidative stress and inflammation in rats. Oxidative Medicine and Cellular Longevity 2017; 2017: 1092015–1092027.
17. Liu W, Gong W, He M, Liu Y, Yang Y, Wang M, Wu M, Guo S, Yu Y, Wang X, Sun F, Li Y, Zhou L, Qin S and Zhang Z. Spironolactone Protects against Diabetic Cardiomyopathy in Streptozotocin-Induced Diabetic Rats. Journal of Diabetes Research 2018; 2018: 9232065–9232077.
18. Hasan R, Abo labanb G, Bakera F, Abdel gawada SK and Hussain A. Comparative study on the effect of live bees' stings versus their venom on a model of hepatic fibrosis in albino rats: a histological and immunohistochemical study. The

Egyptian Journal of Histology 2015; 38: 742–755.

19. Afsar T, Razak S, Khan M and Almajwal A. Acacia hydaspica ethyl acetate extract protects against cisplatin-induced DNA damage, oxidative stress, and testicular injuries in adult male rats. BMC Cancer 2017; 17(1): 883–896.
20. Saad MI, Kamel MA, Hanafi MY, Helmy MH and Shehata RR. Effect of sitagliptin and glimepiride on glucose homeostasis and cAMP levels in peripheral tissues of HFD/STZ diabetic rats. The American Journal of Biomedical Research 2014; 2(3): 52-60.
21. Subhasree N, Kamella A, Kaliappan I, Agrawal A and Dubey GP. Antidiabetic and antihyperlipidemic activities of a novel polyherbal formulation in high fat diet/streptozotocin induced diabetic rat model. Indian journal of pharmacology 2015; 47(5): 509–513.
22. Abdulmalek SA and Balbaa M. Synergistic effect of nano-selenium and metformin on type 2 diabetic rat model: Diabetic complications alleviation through insulin sensitivity, oxidative mediators, and inflammatory markers. PlOS one 2019; 14(8): e0220779-e0220806.
23. Madiraju AK, Erion DM, Rahimi Y, Zhang XM, Braddock DT, Albright RA, Prigaro BJ, Wood JL, Bhanot S and MacDonald MJ. Metformin suppresses gluconeogenesis by inhibiting mitochondrial glycerophosphate dehydrogenase. Nature 2014; 510(7506): 542-546.
24. Im I, Jang M, Park SJ, Lee SH, Choi JH, Yoo HW, Kim S and Han YM. Mitochondrial respiratory defect causes dysfunctional lactate turnover via AMP-activated protein kinase activation in human-induced pluripotent stem cell-derived hepatocytes. J. Biol. Chem. 2015; 290(49): 29493–29505.
25. Diao J, Wei J, Yan R, Fan G, Lin L and Chen M. Effects of resveratrol on regulation on UCP2 and cardiac function in diabetic rats. J Physiol Biochem. 2019; 75(1): 39-51.
26. Wu Z, Huang A, Yan J, Liu B, Liu Q, Zhang J, Zhang X, Ou C and Chen M. Resveratrol ameliorates cardiac dysfunction by inhibiting apoptosis via the PI3K/ Akt/FoxO3a pathway in a rat model of diabetic cardiomyopathy. J. Cardiovasc. Pharmacol. 2017; 70(3): 184-193.
27. Bhattacharjee N, Barma S, Konwar N, Dewanjee S and Manna P. "Mechanistic insight of diabetic nephropathy and its pharmacotherapeutic targets: an update". European Journal of Pharmacology 2016; 791: 8–24.
28. Al-Damry NT, Attia HA, Al-Rasheed NM, Al-Rasheed NM, Mohamad RA, Al-Amin MA and Atteya M. Sitagliptin attenuates myocardial apoptosis via activating LKB-1/AMPK/Akt pathway and suppressing the activity of GSK-3β and p38α/MAPK in a rat model of diabetic cardiomyopathy. Biomedicine & Pharmacotherapy 2018; 107: 347-358.
29. Kobashigawa LC, Xu YC, Padbury JF, Tseng YT and Yano N. Metformin protects cardiomyocyte from doxorubicin induced cytotoxicity through an AMP-activated protein kinase dependent signaling pathway: an in vitro study. PLOS One 2014; 9(8): e104888-e104899.
30. Manjunatha S, Shaik AH, Al Omar SY, Mohammad A and Kodidhela LD. Combined cardio-protective ability of syringic acid and resveratrol against isoproterenol induced cardiotoxicity in rats via attenuating NF-kB and TNF-α

pathway. Sci Rep. 2020; 10(1): 3426-3438.

31. Maritim AC, Sanders RA and Watkins JB. Diabetes, oxidative stress, and antioxidants: a review. J Biochem Mol Toxicol. 2003; 17(1): 24-38.
32. Xu J, Liu LQ, Xu LL, Xing Y and Ye S. Metformin alleviates renal injury in diabetic rats by inducing Sirt1/FoxO1 autophagic signal axis. Clin Exp Pharmacol Physiol. 2020; 47(4): 599-608.
33. Gong L, Guo S and Zou Z. Resveratrol ameliorates metabolic disorders and insulin resistance in high fat diet-fed mice. Life Sciences 2020; 242: 117212-117219.
34. El-Missiry MA, Amer MA, Hemieda FA, Othman AI, Sakr DA and Abdulhadi HL. Cardioameliorative effect of punicalagin against streptozotocin induced apoptosis, redox imbalance, metabolic changes, and inflammation. Egypt. J. Basic Appl. Sci. 2015; 2(4): 247–260.
35. Hsu CP, Zhai P, Yamamoto T, Maejima Y, Matsushima S, Hariharan N, Shao D, Takagi H, Oka S and Sadoshima J. Silent information regulator 1 Sirt1 protects the heart from ischemia/reperfusion. Circulation 2010; 122(21): 2170-2182.
36. Zheng W, Li D, Gao X, Zhang W and Robinson BO. Carvedilol alleviates diabetic cardiomyopathy in diabetic rats. Experimental and Therapeutic Medicine 2019, 17(1): 479–487.
37. Pappachan JM, Varughese GI, Sriraman R and Arunagirinathan G. Diabetic cardiomyopathy: pathophysiology, diagnostic evaluation, and management. World J. Diabetes 2013; 4(5): 177–189.
38. Huynh K, Bernardo B, McMullen J and Ritchie RH. Diabetic cardiomyopathy: mechanisms and new treatment strategies targeting antioxidant signaling pathways. Pharmacology & Therapeutics 2014; 142(3): 375–415.
39. Abdel-Hamid A and Firgany A. Favorable outcomes of metformin on coronary microvasculature in experimental diabetic cardiomyopathy. Journal of Molecular Histology 2018; 49(6): 639–649.
40. Asensio-López M, Lax A, Pascual-Figal D, Valdés M and Sánchez-Más J. Metformin protects against doxorubicin-induced cardiotoxicity: involvement of the adiponectin cardiac system. Free Radical Biology and Medicine 2011; 51(10): 1861–1871.
41. Li P, Shibata R, Unno K, Shimano M, Furukawa M, Ohashi T, Cheng X, Nagata K, Ouchi N and Murohara T. Evidence for the importance of adiponectin in the cardioprotective effects of pioglitazone. Hypertension 2010; 55(1): 69–75.
42. Yang F, Qin Y, Wang Y, Meng S, Xian H, Che H, Lv J, Li Y, Yu Y, Bai Y and Wang L. Metformin Inhibits the NLRP3 Inflammasome via AMPK/mTOR-dependent Effects in Diabetic Cardiomyopathy. International journal of biological sciences 2019; 15(5): 1010–1019.
43. Duarte-Vazquez M, Solis A, Esparza J, Rosado JL and Fragoso LR. Resveratrol Combined with Pioglitazone Ameliorates Cardiovascular Complications in db/db Diabetic Mice. Journal of Metabolic Syndrome 2018; 7(2): 243–249.
44. Arafa M, Mohammad N, Atteia H and Abd-Elaziz HR. Protective effect of resveratrol against doxorubicin-induced cardiac toxicity and fibrosis in male experimental rats. Journal of Physiology and Biochemistry 2014; 70(3): 701–711.

45. Vasamsetti S, Karnewar S, Gopoju R, Gollavilli PN, Narra SR, Kumar JM and Kotamraju S. Resveratrol attenuates monocyte-to-macrophage differentiation and associated inflammation via modulation of intracellular GSH homeostasis: Relevance in atherosclerosis. Free Radical Biology and Medicine 2016; 96: 392–405.